Asian Journal of Chemistry; Vol. 35, No. 10 (2023), 2365-2374

ASIAN JOURNAL OF CHEMISTRY

https://doi.org/10.14233/ajchem.2023.28130

Computational Analysis of Excited State Intramolecular Hydrogen Atom Transfer and Microsolvation Studies on 8-Acetyl-7-hydroxy-4-methylcoumarin using DFT and TDDFT

JAGADEESHA K[1,*], M. PREMSINGH[2], R.J. ANILKUMAR[3] and Y.L. RAMU[4]

[1]Department of Physics, Government College (Autonomous), Mandya-571401, India
[2]Department of Computer Science, Government College (Autonomous), Mandya-571401, India
[3]Department of Computer Science, Maharani Science College for Women (Autonomous), Mysore-570005, India
[4]Department of Physics, Government PU College for Girls, Koppa, Mandya-571425, India

*Corresponding author: E-mail: jageethasha.physics@gmail.com

Received: 8 June 2023; *Accepted*: 20 July 2023; *Published online*: 28 September 2023; AJC-21385

The computational calculations were carried out on 8-acetyl-7-hydroxy-4-methyl coumarin (AHM) and its water complex AHM+$(H_2O)_4$-[AHMH] at ground and excited states by employing density functional theory (DFT)/specific state time-dependent density functional theory (SS-TDDFT). In AHM and AHMH molecules, there is an intramolecular hydrogen bond between hydroxyl group and acetyl group along with inter-molecular hydrogen bonds in the hydrated molecule. The computational studies of molecular structural parameters, molecular electrostatic potential, natural bond orbital (NBO) analysis, the molecular orbital's and UV-Vis spectra of both the molecules under polar solvents were explored by B3LYP/cc-pVDZ/PCM/EFP1 method. The intramolecular hydrogen atom transpired between hydroxyl to acetyl group in AHM/AHMH molecules from $S_0 \rightarrow S_1$ state but not in $S_0 \rightarrow S_3/S_0 \rightarrow S_2$ states even though the S_3/S_2 states have significant oscillation strengths. This indicates that intramolecular charge transfer (ICT) occurs within the molecules and it confirmed using potential energy surface (PES) scan studies.

Keywords: Specific state time-dependent density functional theory, Polarizable continuum model, Intramolecular charge transfer.

INTRODUCTION

The phenomenon of hydrogen bonding has been illustrious for its eminence in various fields like photo-physics, photo-chemistry and biochemistry. The systematic study of hydrogen bonds is much essential for comprehending the photo-physical properties of some organic molecules which is having electron donor and acceptor demeanor at ground and excited states [1-4]. The effective fragment potential (EFP) method furnish a polarizable QM-based force field to characterize the intermolecular interactions. To study the microsolvation effect on biological or organic molecule, EFP1/DFT method was established explicitly for solvation and it interfaced with the polarizable continuum model (PCM) [5,6] and also EFP1/TDDFT method has been fostered for characterizing the electronically excited states of solvated molecules [5,7-9]. In order to enlighten the electronic, molecular, structural and photo-physical properties of many organic and biological molecules time-dependent density functional theory (TDDFT) computations are done at the excited states. At the excited state, refashioning of molecular structure take place within the molecule along with hydrogen transfer. The revamp of hydrogen bond anatomy due to microsolvation effect is to evince the ESIPT/ESIHT process in some organic and biological molecules [10]. The intra-molecular charge transfer (ICT) character correlated with ESIPT/ESIHT is associated to the photo-physical features of biologically active molecules [11].

8-Acetyl-7-hydroxy-4-methyl coumarin (AHM) exhibits anti-coagulant activity due to acetyl group across C8 position of coumarin moiety [12] and also it can empowers the determination of the chemical group responsible for inspiring a target biological effect in the organism. AHM compound exhibits anti-proliferative and cytotoxic activity to suppress cell growth, especially the growth of malignant cells into surrounding tissue [13]. Several metal complexes with AHM shows anti-oxidative and anti-tumour property [14]. In the present theoretical study,

the DFT/TDDFT/EFP1 methods were used to investigate AHM and AHMH molecules in both ground and excited states and also the electronic structure, ICT states of the molecules along with the excited-state intra-molecular hydrogen transfer (ESIHT) process have been explored.

COMPUTATIONAL METHODS

Avogadro software [15] was used to simulate the molecular structures of 8-acetyl-7-hydroxy-4-methyl coumarin (AHM) and its water complex AHM+$(H_2O)_4$ (AHMH) molecules and NBO [16] integrated GAMESS [17,18] was used to execute the computational computations. The geometrical structures of both molecules have been extensively optimized at ground/excited states employing Becke, 3-parameter, Lee-Yang-Parr (B3LYP) [19,20] hybrid functional and cc-pVDZ basis set [21] *via* applying DFT [22-26]/SS-TDDFT [27,28] methods with MMFF94s force field [29]. Both molecules' behaviour in polar solvents like water and ethanol was simulated using PCM [6, 30] and the UV-Vis absorption spectra were computed using SS-TDDFT/cc-pVDZ/B3LYP/PCM/EFP1 [31-33]. At the (S_0, S_1 and S_3)/(S_0, S_1 and S_2) states, the natural charges on various atoms and groups of AHM/AHMH molecules were estimated. Using optimized structural parameters, the energies of the molecules' frontier molecular orbitals/chemical reactive sites were determined by displaying molecular orbitals/MEP visualization. At the S_1 state of AHM and AHMH molecules, an intra-molecular hydrogen atom was transferred from the hydroxyl group to the acetyl group. The ESIHT mechanism was confirmed using a PES maps along the hydrogen bonding's O14-H18···O15=C11/C3= O14···H18-O15 at the DFT/cc-pVDZ/B3LYP/SS-TDDFT level.

RESULTS AND DISCUSSION

Molecular structure at ground and excited states: AHM molecule with 26 atoms, in which methyl (-CH_3), hydroxyl (-OH) and acetyl groups (-$COCH_3$) are attached to the C4, C7 and C8 positions of the basic coumarin moiety. The hydroxyl and acetyl groups are linked by an intra-molecular hydrogen bond and there are also intermolecular hydrogen bonds in the AHMH molecule. Figs. 1 and 2 display the optimized molecular structures as well as the number of atoms in the ground and excited states. Using the DFT/TDDFT/B3LYP approach with the cc-pVDZ basis set, the optimized geometrical parameters of the AHM and their water complex molecule were calculated in the ground and excited states. The results are shown in Table-1. One intra-molecular hydrogen bond O16-H17···O15=C10 connects the oxygens in the hydroxyl (O16-H17) and carbonyl (C10=O15) groups of the AHM molecule. However, in AHMH molecule, in addition to an intra-molecular hydrogen bond, there are four inter-molecular hydrogen bonds and one hydrogen bond exist between molecules of water. One hydrogen bond (WB1) and two inter-molecular hydrogen bonds (HB) will form

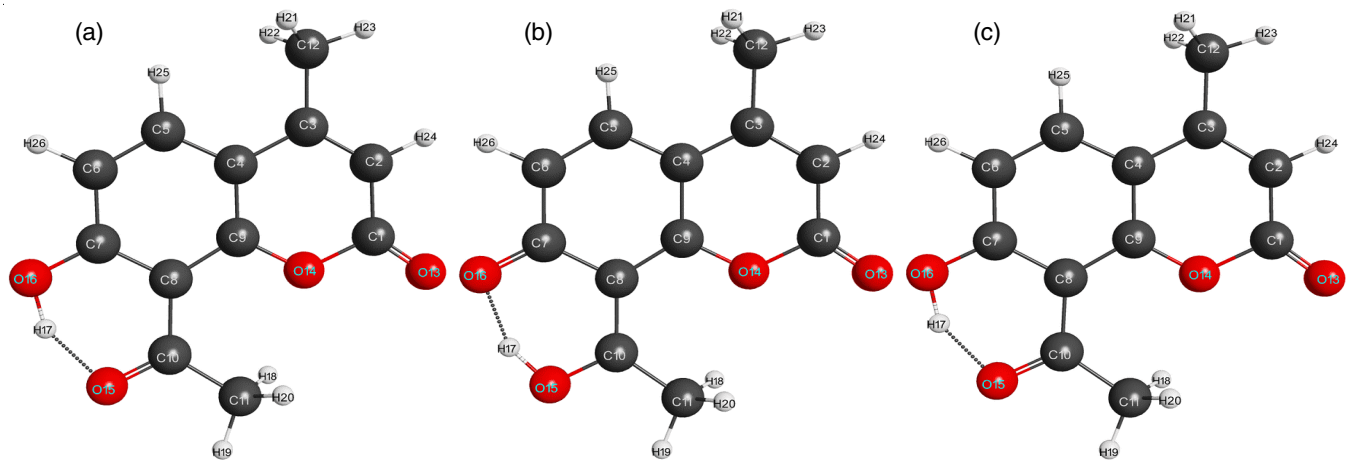

Fig. 1. Optimized molecular structure of AHM molecule at S_0, S_1 and S_3 [(a), (b) and (c)]

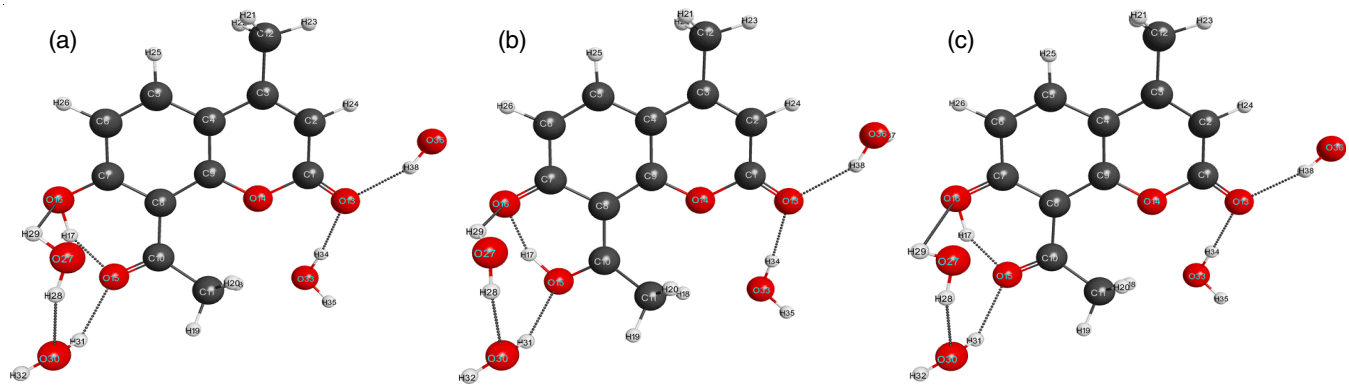

Fig. 2. Optimized molecular structure of AHMH molecule at S_0, S_1 and S_2 [(a), (b) and (c)]

TABLE-1
SELECTED BOND LENGTHS - r (Å) AND BOND ANGLES – A (°) OF AHM AND AHMH MOLECULES IN THE GROUND AND EXCITED STATES

r(Å)/A(°)	AHM			AHMH		
	S_0	S_1	S_3	S_0	S_1	S_2
R(1-2)	1.447	1.442	1.422	1.440	1.440	1.418
R(2-3)	1.363	1.380	1.397	1.366	1.379	1.404
R(3-4)	1.452	1.424	1.443	1.449	1.426	1.458
R(4-5)	1.416	1.402	1.414	1.416	1.401	1.418
R(5-6)	1.378	1.388	1.383	1.377	1.390	1.379
R(6-7)	1.413	1.445	1.415	1.413	1.440	1.426
R(7-8)	1.432	1.457	1.436	1.429	1.454	1.443
R(8-9)	1.422	1.394	1.419	1.417	1.387	1.413
R(8-10)	1.483	1.465	1.459	1.484	1.467	1.484
R(10-11)	1.508	1.492	1.513	1.500	1.487	1.497
R(3-12)	1.505	1.506	1.500	1.505	1.506	1.494
R(4-9)	1.411	1.480	1.439	1.410	1.476	1.439
R(1-13)	1.205	1.209	1.216	1.222	1.221	1.234
R(1-14)	1.416	1.407	1.449	1.391	1.389	1.439
R(9-14)	1.355	1.352	1.351	1.362	1.360	1.362
R(10-15)	1.245	1.331	1.269	1.247	1.336	1.254
R(7-16)	1.326	1.270	1.328	1.329	1.276	1.426
R(15-17)	–	1.029	–	–	1.032	–
R(17-16)	1.011	–	1.015	1.010	–	1.032
R(2-24)	1.091	1.090	1.084	1.090	1.089	1.092
R(12-21)	1.103	1.102	1.110	1.103	1.102	1.108
R(12-22)	1.103	1.098	1.100	1.103	1.102	1.100
R(12-23)	1.098	1.098	1.093	1.098	1.098	1.110
R(5-25)	1.091	1.090	1.084	1.091	1.090	1.090
R(6-26)	1.090	1.092	1.084	1.091	1.092	1.090
R(11-18)	1.100	1.104	1.093	1.098	1.101	1.099
R(11-19)	1.097	1.099	1.091	1.098	1.100	1.098
R(11-20)	1.100	1.104	1.093	1.100	1.105	1.100
A(1-2-3)	122.7	122.5	124.0	121.6	121.6	124.0
A(2-3-4)	119.3	119.2	117.5	119.3	119.2	115.6
A(3-4-9)	118.6	118.9	119.4	118.7	118.9	120.2
A(4-9-14)	120.4	118.7	121.0	120.1	118.6	121.3
A(9-14-1)	123.7	123.8	121.9	123.1	122.9	119.8
A(14-1-2)	115.4	116.9	116.2	117.1	118.3	118.1
A(14-1-13)	116.5	116.2	114.0	115.9	115.7	113.1
A(2-1-13)	128.1	127.0	129.8	127.0	126.0	128.8
A(2-3-12)	120.7	120.0	121.5	120.5	119.9	122.6
A(4-3-12)	120.0	120.8	121.0	120.3	120.9	121.7
A(4-5-6)	121.8	120.0	121.8	121.6	120.1	122.1
A(5-6-7)	120.2	123.1	120.3	120.2	122.6	119.8
A(6-7-8)	120.5	118.7	120.9	120.6	118.9	120.7
A(7-8-9)	117.2	116.8	117.2	117.1	116.9	117.5
A(8-9-4)	122.5	123.9	122.2	122.6	123.7	122.0
A(5-4-9)	117.8	117.5	117.6	117.7	117.4	117.8
A(9-8-10)	125.0	124.5	125.1	125.0	124.5	125.4
A(7-8-10)	117.9	118.6	117.7	117.8	118.6	117.1
A(8-10-15)	119.2	118.3	119.2	118.6	117.3	118.2
A(16-7-8)	122.1	121.9	121.9	121.9	121.2	121.9
A(17-16-7)	105.3	–	106.5	104.6	–	104.6
A(15-10-11)	117.3	114.4	116.0	118.3	116.1	118.4
A(8-10-11)	123.4	127.3	124.7	123.0	126.4	123.3
A(16-7-6)	117.3	119.3	117.2	117.5	119.8	117.4

between the oxygen of the hydroxyl and carbonyl groups and two HBs will form across the keto group of the pyrone ring of the coumarin molecule.

When AHM is photo-excited, the structural characteristics such as bond angles and bond lengths are changed in both the S_1 and S_3 excited states. In the S_1 state, the C3-C4 and C8-C9 bond lengths get reduced by 0.028 Å, while the C1-C2/C8=C10 bond lengths are substantially decreased by 0.025/0.024 Å in the S_3 state. The C6-C7/C7-C8/C4=C9/C10-O15 bond lengths are elongated by 0.032/0.025/0.069/0.086 Å in S_1 state and C6-C7/C4=C9/C10-O15 bond lengths are elongated by 0.034/0.028/0.024 Å in S_3 state. In both excited states, the other bond lengths vary in the (1-3) × 10^{-3} Å range. The bond angles between the atoms of an AHM molecule vary in the range (0.1-3.9)°/(0-2.5)° in the S_1/S_3 states. Because of the action of microsolvation, structural characteristics such as bond angles and bond lengths are altered. The C1-O14 bond length was reduced by 0.025 Å, whereas C1=O13 bond length was raised by 0.017 Å. Other bond lengths vary from (1-3) × 10^{-3} Å. The bond angles between the atoms of the AHMH molecule range from (0-1.7)°. When AHMH is photo-excited, structural properties such as bond angles and bond lengths are changed in both the S_1 and S_3 states. Here, C10-C11 bond length dropped by 0.013 Å in the S_1 state and 0.003 Å in the S_2 state. Bond lengths of C6-C7/C7-C8/C4-C9/C10-O15 are elevated by 0.027/0.025/0.066/0.089 Å in S_1 and 0.038/0.013/0.014/0.029 Å in S_2.

Hydrogen bond dynamics: The photophysical characteristics of AHM and AHMH molecules are affected by both intra- and inter-molecular HB-bonding. The computational study on AHM and AHMH molecules at DFT/TDDFT level using cc-pVDZ/B3LYP approach has been established to sketch the complete picture of both intra-molecular and inter-molecular hydrogen bonds at the ground and excited states. An intra-molecular HB O16-H17···O15=C10 with a length of 1.549 Å will occur between the hydroxyl and acetyl group in the ground state of AHM/AHMH molecules. However, due to a hydrogen atom transfer from the hydroxyl to the acetyl group at the S_1 state of AHM/AHMH, this intra-molecular HB is transformed as O15-H17···O16=C7 of length 1.514/1.513 Å. There is no hydrogen atom transfer from the hydroxyl to the acetyl group in S_3/S_2 states that have high oscillation strengths in AHM/AHMH molecules. However, the intra-molecular HB length of AHM molecule in the S_3 state changes from 1.549 Å to 1.521 Å, while AHMH molecule in the S_2 state changes from 1.549 Å to 1.488 Å.

In AHMH molecule, two inter-molecular hydrogen bonds were formed across the 2-pyrone molecule, two more inter-molecular hydrogen bonds were formed between the hydroxyl and acetyl groups and one HB was formed between the water molecules. When AHM and AHMH molecules are photo-excited, the intra-molecular HB O16-H17···O15=C10 length in AHM decreases by 0.035 Å/0.028 Å in S_1/S_3 states due to a decrease/increase in charge on H17 by 0.002e/0.015e and an increase in charge on O15 by -0.051e and -0.004e in S_1 and S_3 states. In AHMH molecule, the intra-molecular HB O16-H17···O15=C10 length drops by 0.036 Å/0.061 Å in S_1/S_2 states due to a reduction/rise in charge on H17 by 0.005e/0.013e and an increase in charge on O15 by -0.046e and -0.003e in S_1 and S_2 states, respectively.

Microsolvation has no influence on intra-molecular HB length. The inter-molecular HBs C1=O13···H38-O36 and

TABLE-2
INTRA-MOLECULAR AND INTER-MOLECULAR HB LENGTHS OF AHM AND AHMH MOLECULES AT GROUND AND EXCITED STATES

r (Å)	HB lengths (Å)					
	AHM			AHMH		
	S_0	S_1	S_3	S_0	S_1	S_2
O16-H17···O15=C10/O15-H17···O16=C7	1.549	1.514	1.521	1.549	1.513	1.488
C7=O16···H29-O27/O16-H17···O27=H28	–	–	–	2.294	1.994	2.449
C10=O15···H31-O30	–	–	–	1.922	1.920	1.931
C1=O13···H38-O36	–	–	–	1.872	1.915	1.851
C1=O13···H34-O33	–	–	–	1.841	1.859	1.827
O27-H28···O30-H31(WB)	–	–	–	1.842	1.853	1.819

TABLE-3
DIHEDRAL ANGLES -A (°) ACROSS INTRA-MOLECULAR AND INTER-MOLECULAR HB LENGTH'S OF AHM AND AHMH MOLECULES AT GROUND AND EXCITED STATES

r (Å)	Dihedral angle -A (°)					
	AHM			AHMH		
	S_0	S_1	S_3	S_0	S_1	S_2
O16-H17···O15=C10/O15-H17···O16=C7	- 0.1	0.1	0	2.5	22	12.7
C7=O16···H29-O27/O16-H17···O27=H28	–	–	–	-58.6	-51.3	155.9
C10=O15···H31-O30	–	–	–	78.2	74.3	81.3
C1=O13···H38-O36	–	–	–	-22.5	-10.3	-41.0
C1=O13···H34-O33	–	–	–	2.9	3.2	-22.8
O27-H28···O30-H31 (WB)	–	–	–	-7.4	7.7	-0.2

C1=O13···H34-O33 across the 2-pyrone of AHMH molecule extended by 0.043 Å and 0.018 Å in the S_1 state due to a -0.059e drop in charge on O13, but decreased by 0.064 Å and 0.014 Å in the S_2 state. The inter-molecular HB C10=O15···H31-O30 across acetyl group decreased/extended in length by 0.002 Å/ 0.009 Å in S_1/S_2 states due to a -0.046e/-0.003e rise in charge on O15. Furthermore, the inter-molecular HB C7=O16···H29-O27 length decreased by 0.3 Å in the S_1 state and changed to O16-H17···O27=H28 in the S_2 state, with its length increasing by 0.155 Å due to a -0.016e/-0.092e drop in charge on O16 in the S_1/S_2 states. The HB O27-H28···O30–H31 in between water molecules elongates/shortens by 0.011 Å/0.023 Å in S_1/S_2 states. Tables 2 and 3 show the intra-molecular and inter-molecular HB lengths, as well as the dihedral angles across HBs that correspond to AHM and AHMH molecules at ground and excited states.

Natural charge analysis and ESIHT process: By employing the NBO 6.0 package, which was integrated into the GAMESS programme, the natural charges on hydroxyl/acetyl/ methyl groups and on different atoms of AHM and AHMH molecules at both the ground and excited states were computed at the DFT/TDDFT/B3LYP/cc-pVDZ level and given in Table-4. The total natural charge of the benzene ring/pyrone ring/hydroxyl groups/acetyl group/methyl group in the ground state of AHM and AHMH molecules is -0.047e/0.181e/-0.156e/0.016e/ 0.064e and -0.012e/0.214e/-0.166e/0.031e/-0.067e, respectively. As a result of the micro-solvation effect, the total natural charge on the benzene ring fell by -0.035e, while it increased on the pyrone ring, hydroxyl groups, acetyl groups and methyl groups by 0.004e, 0.033e, -0.01e, 0.015e and 0.003e, respectively.

The natural charge on each atom varies due to the photo-excitation of the AHM molecule. In S_1 state, natural charge on

TABLE-4
NATURAL CHARGES ON DIFFERENT ATOMS OF AHM AND AHMH MOLECULES AT GROUND AND EXCITED STATES

Atomic number	AHM			AHMH		
	S_0	S_1	S_3	S_0	S_1	S_2
C1	0.778	0.768	0.758	0.792	0.786	0.709
C2	-0.354	-0.315	-0.378	-0.361	-0.316	-0.335
C3	0.050	0.036	0.069	0.060	0.043	-0.070
C4	-0.176	-0.103	-0.178	-0.172	-0.098	-0.036
C5	-0.159	-0.225	-0.167	-0.158	-0.219	-0.186
C6	-0.288	-0.196	-0.306	-0.283	-0.191	-0.233
C7	0.429	0.427	0.435	0.438	0.433	0.461
C8	-0.273	-0.278	-0.286	-0.252	-0.262	-0.213
C9	0.420	0.443	0.434	0.415	0.440	0.359
C10	0.576	0.404	0.570	0.617	0.430	0.596
C11	-0.718	-0.702	-0.757	-0.742	-0.725	-0.743
C12	-0.667	-0.668	-0.716	0.669	-0.670	-0.671
O13	-0.552	-0.497	-0.555	-0.658	-0.599	-0.658
O14	-0.537	-0.518	-0.520	-0.520	-0.511	-0.545
O15	-0.606	-0.657	-0.610	-0.651	-0.697	-0.654
O16	-0.668	-0.642	-0.678	-0.680	-0.664	-0.588
H17	0.512	0.510	0.527	0.514	0.509	0.527
H18	0.260	0.244	0.272	0.320	0.300	0.331
H19	0.245	0.245	0.261	0.236	0.238	0.234
H20	0.259	0.244	0.271	0.251	0.240	0.256
H21	0.244	0.249	0.260	0.245	0.251	0.227
H22	0.244	0.249	0.259	0.244	0.249	0.223
H23	0.243	0.243	0.258	0.247	0.248	0.246
H24	0.250	0.254	0.265	0.281	0.296	0.269
H25	0.239	0.240	0.250	0.239	0.242	0.247
H26	0.249	0.246	0.263	0.247	0.247	0.249

O15 increases to a greater degree (-0.051e) than in S_3 state, whereas natural charge on O16/H17 falls to a greater extent (-0.026e/0.002e). As a result, intra-molecular charge transfer takes place *i.e.* transfer of hydrogen atom (H17) from a hydroxyl

group to an acetyl group results in an intra-molecular HB change from O16-H17···O15=C10 to O15-H17···O16=C7 in the S_1 state but not in the S_3 state. Similar to this, each atom's natural charge changes as a result of the AHMH molecule being photo-excited. The natural charge on O15 grows more in the S_1 state (-0.046e) compared to the S_2 state and the natural charge on O16 and H17 falls more (-0.016e and 0.005e), respectively. Thus, intra-molecular charge transfer occurs, specifically, when hydrogen atom (H17) transfer from hydroxyl to acetyl group with adjustment of intra-molecular HB O16-H17···O15=C10 as O15-H17···O16=C7 in S_1 state but not in S_2 state.

UV-Vis spectral studies: TDDFT/PCM/EFP1/B3LYP/cc-pVDZ method was used to compute the electronic absorption spectra of AHM and AHMH molecules. Fig. 3 depicts the UV-Vis spectra of AHM/AHMH molecules recorded in gas and polar solvents. Using the PCM, the electronic absorption spectra of AHM/AHMH molecules in ethanol, water and gas phases show a band at 340.2 nm, 340 nm and 337.5 nm/333.7 nm, 333.6 nm and 328.8 nm, respectively. Table-5 displays the wavelengths (λ), oscillator strengths (f) and probable wave functions that correspond to significant contributions in gas phase and polar solvents.

The computed absorption wavelength difference demonstrates that solvent effects on AHM molecule create a red shift of 2.5 nm/2.7 nm in water/ethanol and solvent effects on AHMH molecule cause a red shift of 4.8 nm/4.9 nm in water/ethanol. The absorption band shifts to higher wave numbers as the energy gap between the two states narrows. The calculated absorption wavelength of the AHM molecule in the ethanol solvent was approximately 340.2 nm and it is in good agreement with the experimental result, which is approximately 334 nm [34].

Molecular orbital (MO) analysis: The molecular orbitals can be used to investigate the charge transfer characteristics of AHM and AHMH molecules. The most significant MO's of AHM and their water complex are HOMO, HOMO-1, LUMO, LUMO+1 that have been estimated theoretically at DFT/B3LYP/6-31G(d,p) level and are shown in Figs. 4 and 5. The highest occupied orbitals like HOMO/HOMO-1 having energies (-6.2041 eV/-7.2382 eV, -6.2586 eV/-7.2382 eV) and lowest unoccupied

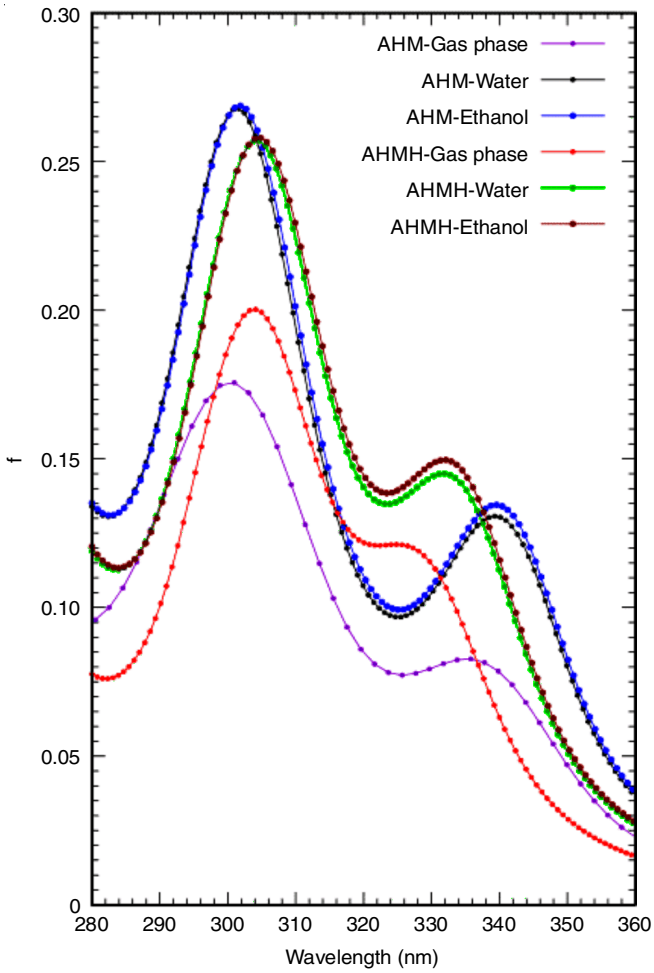

Fig. 3. Simulated absorption spectra of AHM and AHMH molecules in gas phase, water and ethanol solvents

orbitals like LUMO/LUMO+1 having energies (-2.0680 eV/-1.6054 eV, -2.0952 eV/-1.6326 eV) corresponds to AHM and AHMH molecules, respectively. The significant charge transfer mechanism that may occur within the molecules given by [4.1361 eV/5.6328 eV] and [4.1634 eV/5.6056 eV] for AHM and their water complex molecules is explained by the energy

TABLE-5
PEAKS REPRESENTS THE THEORETICAL SIMULATED UV-VIS ABSORPTION SPECTRA WAVELENGTHS (λ) OF AHM AND AHMH MOLECULES CORRESPONDS TO ELECTRONIC TRANSITIONS WITH OSCILLATOR STRENGTHS (f) IN GAS PHASE, IN WATER AND ETHANOL SOLVENTS

Molecule	Solvent/gas phase	State	λ_a (nm)	f	Wave function (excitation amplitude)
AHM	Gas	S_1	337.5	0.0807	H-1→L(-0.152), H-1→L+1(-0.122), H→L(-0.875), H→L+1(0.420)
		S_3	300.5	0.2145	H-1→L(-0.124), H→L(0.427), H→L+1(0.883)
	Water	S_1	340.0	0.1209	H-1→L(-0.135), H-1→L+1(-0.111), H→L(-0.917), H→L+1(-0.333)
		S_2	301.6	0.2701	H-1→L(0.119), H→L(-0.343), H→L+1(0.922)
	Ethanol	S_1	340.2	0.124	H-1→L(-0.135), H-1→L+1(0.110), H→L(-0.918), H→L+1(-0.331)
		S_2	302.0	0.273	H-1→L(0.117), H→L(-0.341), H→L+1(0.923)
AHMH	Gas	S_1	328.8	0.099	H-1→L(0.180), H→L(-0.826), H→L+1(0.499)
		S_2	303.6	0.204	H-1→L(-0.183), H→L(-0.513), H→L+1(-0.821)
	Water	S_1	333.6	0.125	H-1→L(0.152), H→L(-0.880), H→L+1(-0.414)
		S_2	304.3	0.260	H-1→L(-0.152), H→L(-0.426), H→L+1(0.879)
	Ethanol	S_1	333.7	0.128	H-1→L(0.151), H→L(-0.882), H→L+1(-0.411)
		S_2	304.6	0.262	H-1→L(0.152), H→L(0.424), H→L+1(-0.881)

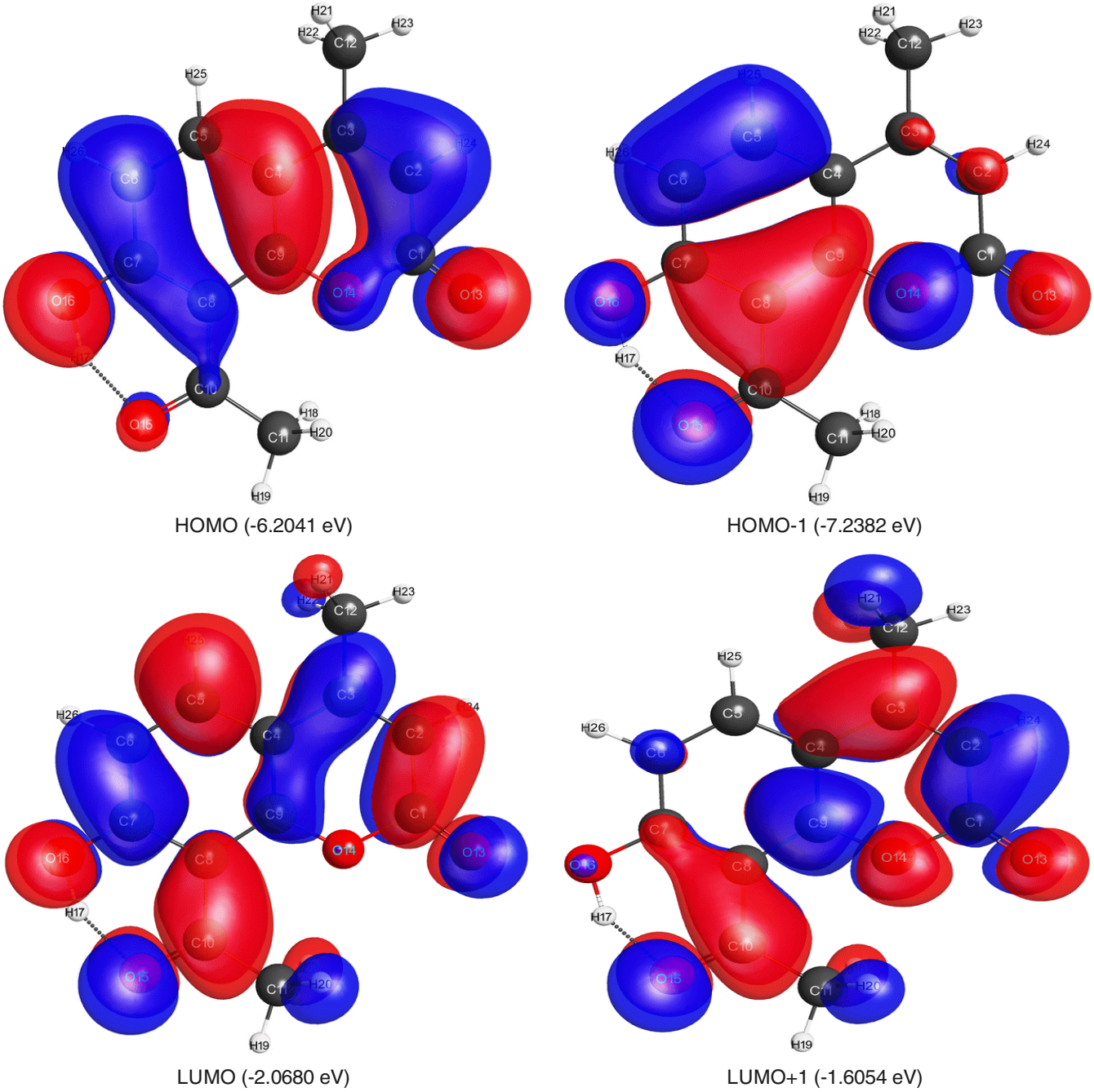

Fig. 4. Molecular orbital images of 8-acetyl-7-hydroxy-4-methyl coumarin (AHM) molecule

difference between [HOMO-LUMO]/[HOMO-1-LUMO+1]. Due to the influence of microsolvation, it is observed that the energy gap between [HOMO-LUMO]/[HOMO-1-LUMO+1] in AHMH is more/smaller by 0.0273 eV/0.0272 eV.

Molecular electrostatic potential (MEP): The MEP representation of AHM and AHMH molecules is computed at the B3LYP/6-31G(d,p) level. By analyzing the plots produced by screening the colours on the surface, one may determine the electrical properties of the molecules. The MEP map (Figs. 6 and 7) displays a spectrum exposure of increasing potential value from red to blue. The electrophilic/nucleophilic spots on the MEP surface and HB interactions can be identified by measuring the electrical density of the molecules under investigation. The negative/positive electrostatic potential zones are primarily localized over the benzene ring, hydroxyl groups/pyrone ring, acetyl group, methyl groups both in AHM and AHMH molecules in ground states. This information was derived from MEP maps. The benzene ring and the hydroxyl group exhibit negative properties in the S_0 state of AHM, whereas the pyrone ring and the acetyl/methyl groups exhibit positive properties.

When AHM is photoexcited, the benzene ring, methyl/pyrone/hydroxyl/acetyl groups change to positive/greater positive/negative/greater negative nature in the S_1 state. In S_3 state, (hydroxyl group, benzene ring)/(pyrone ring and methyl group, acetyl group) turns out (negative, more negative)/(positive,

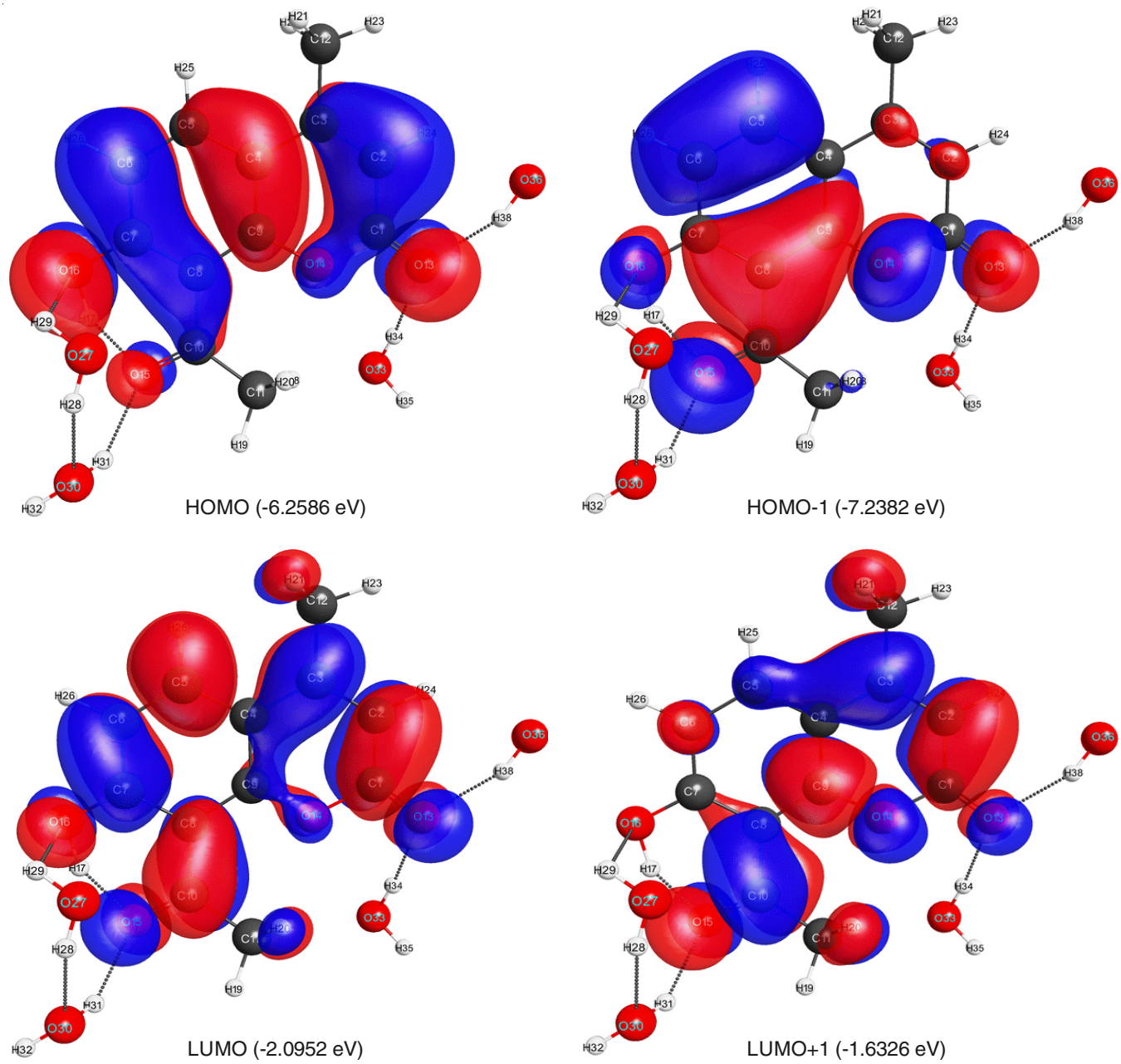

Fig. 5. Molecular orbital images of AHMH molecule

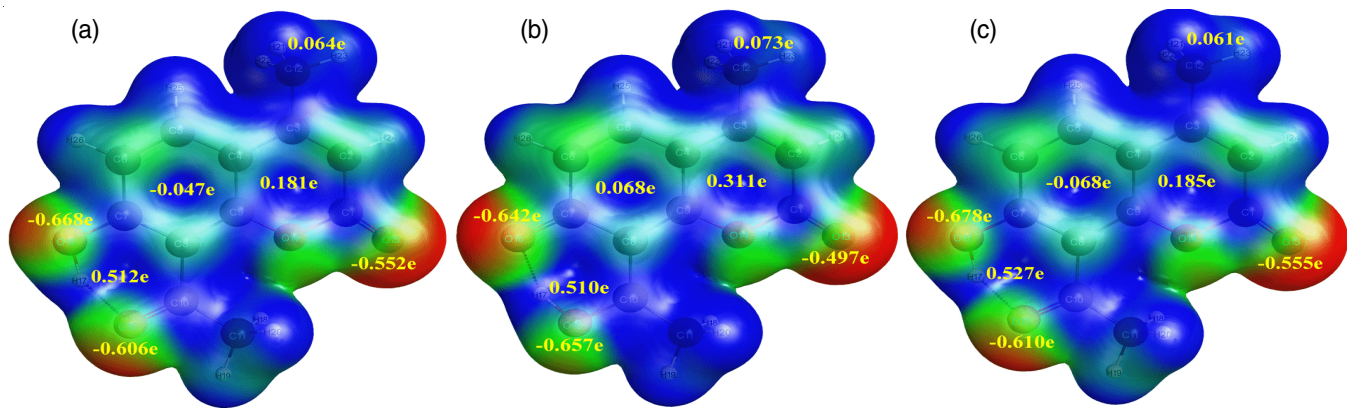

Fig. 6. MEP images with charges on various atoms and groups for AHM molecule at S_0, S_1 and S_3 [(a), (b) and (c)]

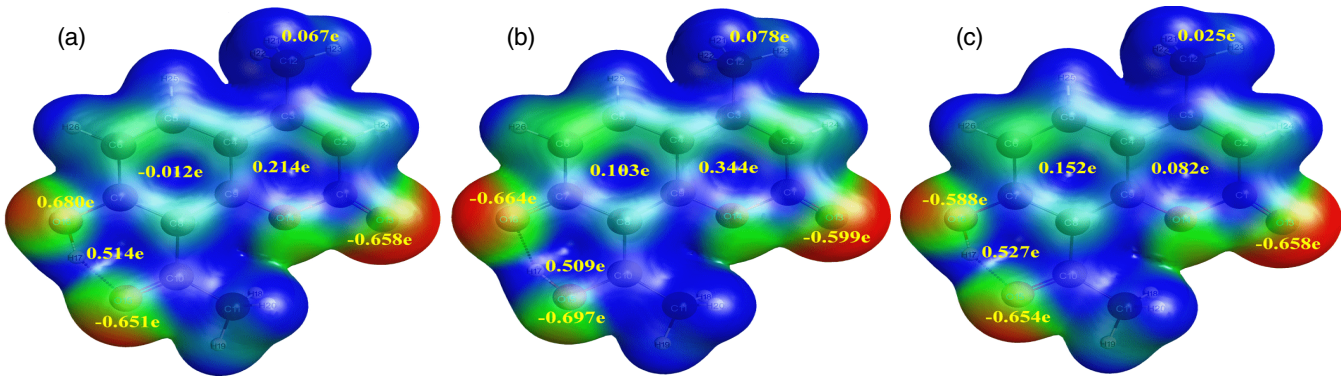

Fig. 7. MEP with charges on various atoms and groups for AHMH molecule at S_0, S_1 and S_2 [(a), (b) and (c)]

remarkably positive). The benzene ring/hydroxy group in the AHMH molecule are negative in nature, while the pyrone, acetyl/methyl group are positive in nature. However, at S_1 benzene ring/acetyl group takes on a more positive/more negative character. Hence, pyrone ring/methyl group gets more favourable. The benzene ring becomes more positive in the S_3 state, whereas the pyrone ring/acetyl group/methyl group becomes less positive. In this case, the hydroxyl group becomes less negative in S_1 state and significantly negative in S_2 state.

ESIHT mechanism: The potential energy surface (PES) scans is an effective approach for investigating the ESIHT mechanism in AHM and AHMH molecules. By taking into account, four alternative states based on constrained relaxed and unrelaxed optimizations in the S_0, S_1, S_3/S_0, S_1, S_2 states of AHM/AHMH molecules, the potential energy curves have been scanned through intra-molecular HB O16-H17···O15=C10. By adjusting the O16-H17 and O15-H17 distances for both molecules from 0.7 to 1.9 Å in steps of 0.02 Å and using the DFT/TDDFT/B3LYP/6-31G(d,p) approach, PES curves may be generated in the gas phase. AHM and AHMH molecules can persist in un-relaxed first excited state (S_1^*) by irradiating with the radiation of energy 4.09 eV and 4.13 eV, the O15-H17 bond extends to 1.575 Å and 1.57 Å respectively, the H17 atom isolated from O15 and embedded to O16. This intersection point corresponds to ESIHT.

The AHM/AHMH molecules sets in the relaxed first excited state S_1 with O15-H17 bond lengths of 1.029 Å/1.032 Å, respectively. The fluorescence may occur in AHM/AHMH molecules with the emission of 2.95 eV/2.88 eV energy. The molecules de-excited to the unrelaxed ground state S_0^*. At this condition, the O16–H17 bond length in AHM/AHMH molecules again elongates to 1.41 Å/1.43 Å, respectively, where hydrogen atom (H17) eviction from O16 to O15 occurs and the molecules regress to their ground state. By generating the PES scan maps (Figs. 8 and 9), it is possible to demonstrate the hydrogen (H17) transfer mechanism that happens in the $S_0 \rightarrow S_1$ state of AHM/AHMH molecules. Furthermore, it is observed that AHM/AHMH molecules excited from $S_0 \rightarrow S_3/S_0 \rightarrow S_2$ states even S_3/S_2 states with high oscillation strengths, do not transfer a hydrogen atom (H17) from the hydroxyl to acetyl group. The non-intersection of PES curves, which were asserted by drawing PES scans as shown in Figs. 10 and 11, serves as confirmation of this non-transfusion of the hydrogen atom.

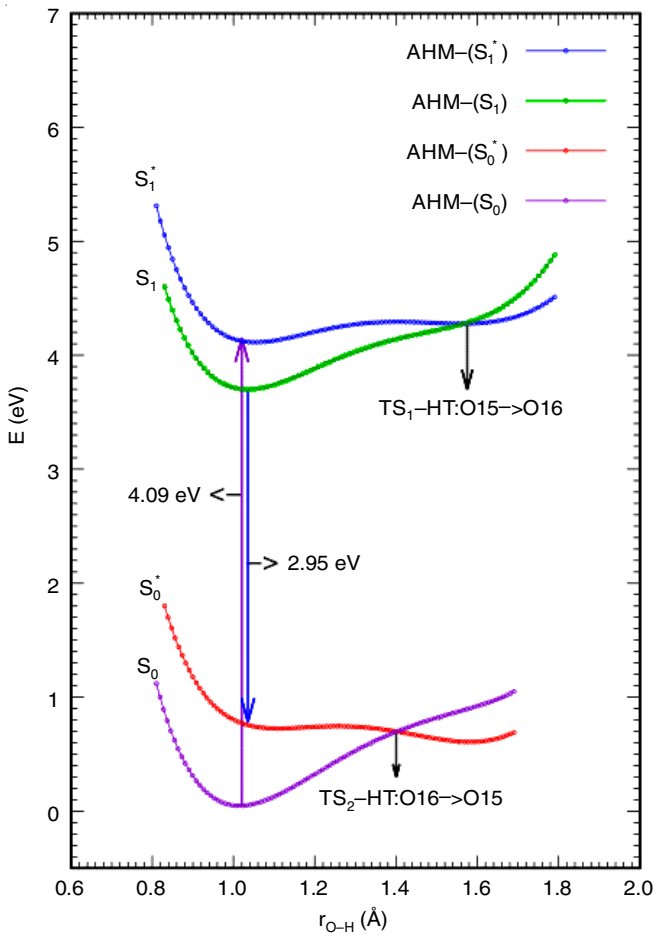

Fig. 8. PES profiles of the O-H bond (O16/15–H17) in AHM molecule at S_0 and S_1 states

Conclusion

This theoretical study employs the density functional theory (DFT) and time-dependent density functional theory (TDDFT) methods, namely the B3LYP functional with the 6-31G(d,p) basis set. The primary objective is to examine the excited-state intramolecular hydrogen transfer (ESIHT) process by conducting potential energy surface (PES) scans in 8-acetyl-7-hydroxy-4-methyl coumarin (AHM) and its water complex AHM+$(H_2O)_4$ (AHMH) molecules. It is observed that the transfer of the hydrogen atom from the hydroxyl to acetyl group induces alterations in the intra-molecular hydrogen bonding (HB) as a

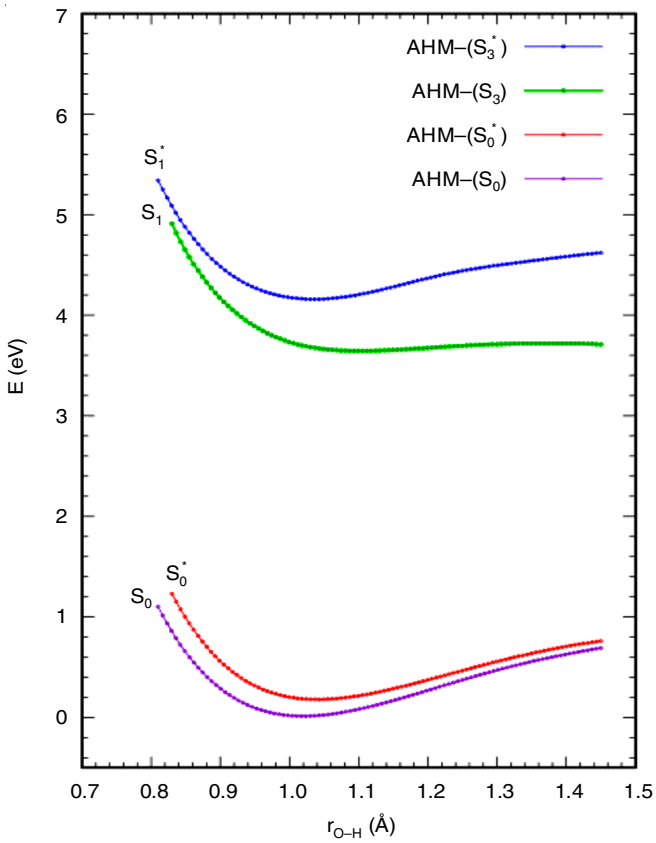

Fig. 9. PES profiles of the O-H bond (O16/15–H17) in AHM molecule at S_0 and S_3 states

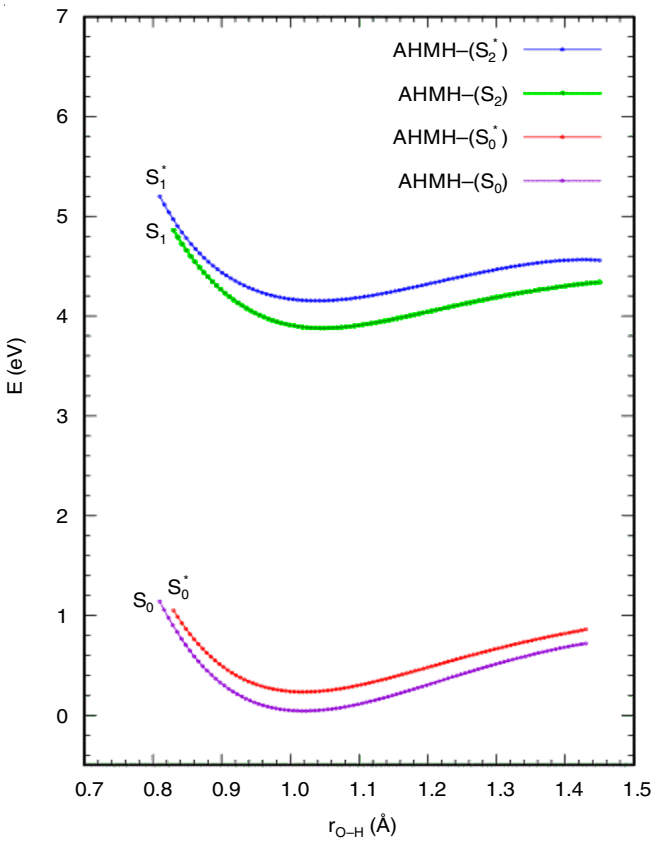

Fig. 11. PES profiles of the O-H bond (O16/15–H17) in AHMH molecule at S_0 and S_2 states

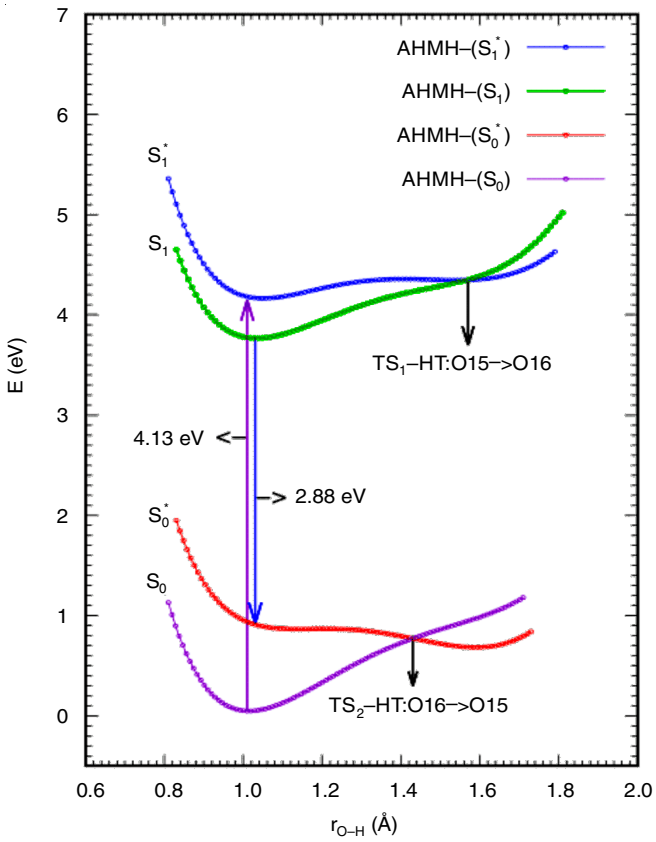

Fig. 10. PES profiles of the O-H bond (O16/15–H17) in AHMH molecule at S_0 and S_1 states

consequence of the excitation of molecules from the $S_0 \rightarrow S_1$ state. When AHM/AHMH molecules are excited from $S_0 \rightarrow S_3$/$S_0 \rightarrow S_2$ states, no hydrogen atom (H17) transfers from the hydroxyl to the acetyl group even though the S_3/S_2 states have significant oscillation strengths. The estimated absorption wavelength of an AHM molecule in ethanol solvent agrees well with the experimental value and a red shift is detected, which corresponds to the $n \rightarrow \pi^*$ transition and is caused by attractive polarization forces between the solute (AHM/AHMH molecules) and polar solvents. The examination of the molecules' intramolecular charge transfer (ICT) state is explained by their molecular orbitals, MEP plots and natural charge computations. The ESIHT mechanism and microsolvation studies allow for continued study on the biological and chemical activity of numerous hydroxy coumarins and their derivatives.

CONFLICT OF INTEREST

The authors declare that there is no conflict of interests regarding the publication of this article.

REFERENCES

1. M. Miao and Y. Shi, *J. Comput. Chem.*, **32**, 3058 (2011); https://doi.org/10.1002/jcc.21888
2. M. Ramegowda, *New J. Chem.*, **37**, 2648 (2013); https://doi.org/10.1039/c3nj00446e
3. M. Ramegowda, *Spectrochim. Acta A Mol. Biomol. Spectrosc.*, **137**, 99 (2015); https://doi.org/10.1016/j.saa.2014.08.017

4. M. Zhang, B. Ren, Y. Wang and C. Zhao, *Spectrochim. Acta A Mol. Biomol. Spectrosc.*, **101**, 191 (2013); https://doi.org/10.1016/j.saa.2012.09.045
5. M. Ramegowda, K.N. Ranjitha and T.N. Deepika, *New J. Chem.*, **40**, 2211 (2016); https://doi.org/10.1039/C5NJ02917A
6. M.S. Gordon, M.A. Freitag, P. Bandyopadhyay, J.H. Jensen, V. Kairys and W.J. Stevens, *J. Phys. Chem. A*, **105**, 293 (2001); https://doi.org/10.1021/jp002747h
7. Y.L. Ramu, K. Jagadeesha, T. Shivalingaswamy and M. Ramegowda, *Chem. Phys. Lett.*, **739**, 137030 (2020); https://doi.org/10.1016/j.cplett.2019.137030
8. S. Sardari, Y. Mori, K. Horita, R.G. Micetich, S. Nishibe and M. Daneshtalab, *Bioorg. Med. Chem.*, **7**, 1933 (1999); https://doi.org/10.1016/S0968-0896(99)00138-8
9. M. Savarese, P.A. Netti, C. Adamo, N. Rega and I. Ciofini, *J. Phys. Chem. B*, **117**, 16165 (2013); https://doi.org/10.1021/jp406301p
10. K. Jagadeesha, Y.L. Ramu, M. Ramegowda and N.K. Lokanath, *Spectrochim. Acta A Mol. Biomol. Spectrosc.*, **208**, 325 (2019); https://doi.org/10.1016/j.saa.2018.10.015
11. K.L. Han and G.J. Zhao, Hydrogen Bonding Transfer in the Excited State, John Wiley & Sons Ltd.: NewYork (2011).
12. R.B. Arora and C.N. Mathur, *Br. J. Pharmacol. Chemother.*, **20**, 29 (1963); https://doi.org/10.1111/j.1476-5381.1963.tb01294.x
13. R. Vázquez, M.E. Riveiro, M. Vermeulen, E. Alonso, C. Mondillo, G. Facorro, L. Piehl, N. Gómez, A. Moglioni, N. Fernández, A. Baldi, C. Shayo and C. Davio, *Bioorg. Med. Chem.*, **20**, 5537 (2012); https://doi.org/10.1016/j.bmc.2012.07.043
14. Q. Zhang, J. Zhai, Y. Zhang, Y. Liu, L. Wang, S.-B. Li, D.-Z. Liao and G.-L. Wang, *Transition Met. Chem.*, **25**, 93 (2000); https://doi.org/10.1023/A:1007036718734
15. M.D. Hanwell, D.E. Curtis, D.C. Lonie, T. Vandermeersch, E. Zurek and G.R. Hutchison, *J. Cheminform.*, **4**, 17 (2012); https://doi.org/10.1186/1758-2946-4-17
16. E.D. Glendening, J.K. Badenhoop, A.E. Reed, J.E. Carpenter, J.A. Bohmann, C.M. Morales, C.R. Landis and F. Weinhold, Theoretical Chemistry Institute, Universityof Wisconsin, Madison, WI (2013).
17. M.W. Schmidt, K.K. Baldridge, J.A. Boatz, S.T. Elbert, M.S. Gordon, J.H. Jensen, S. Koseki, N. Matsunaga, K.A. Nguyen, S.J. Su, T.L. Windus, M. Dupuis and J.A. Montgomery, *J. Comput. Chem.*, **14**, 1347 (1993); https://doi.org/10.1002/jcc.540141112
18. M.S. Gordon and M.W. Schmidt, Advances in Electronic Structure Theory: GAMESS A Decade Later, In: Theory Applications of Computational Chemistry, the First Forty Years, Elsevier, Amsterdam, Chap. 4, pp. 1167-1189 (2005); https://doi.org/10.1016/B978-044451719-7/50084-6
19. A.D. Becke, *J. Chem. Phys.*, **98**, 5648 (1993); https://doi.org/10.1063/1.464913
20. A.D. Becke, *Phys. Rev. A Gen. Phys.*, **38**, 3098 (1988); https://doi.org/10.1103/PhysRevA.38.3098
21. T.H. Dunning Jr., *J. Chem. Phys.*, **90**, 1007 (1989); https://doi.org/10.1063/1.456153
22. R. G. Parr and W. Yang, M, International Academy of Quantum Molecular Science, vol 3. Springer,11(1980); https://doi.org/10.1007/978-94-009-9027-2_2
23. K. Kim and K.D. Jordan, *J. Phys. Chem.*, **98**, 10089 (1994); https://doi.org/10.1021/j100091a024
24. P.J. Stephens, F.J. Devlin, C.F. Chabalowski and M.J. Frisch, *J. Phys. Chem.*, **98**, 11623 (1994); https://doi.org/10.1021/j100096a001
25. T.R. Cundari and W.J. Stevens, *J. Chem. Phys.*, **98**, 5555 (1993); https://doi.org/10.1063/1.464902
26. P.J. Hay and W.R. Wadt, *J. Chem. Phys.*, **82**, 299 (1985); https://doi.org/10.1063/1.448975
27. S. Tokura, T. Sato, T. Tsuneda, T. Nakajima and K. Hirao, *J. Comput. Chem.*, **29**, 1187 (2008); https://doi.org/10.1002/jcc.20871
28. M. Chiba, T. Tsuneda and K. Hirao, *Chem. Phys. Lett.*, **420**, 391 (2006); https://doi.org/10.1016/j.cplett.2006.01.015
29. T.A. Halgren, *J. Comput. Chem.*, **20**, 720 (1999); https://doi.org/10.1002/(SICI)1096-987X(199905)20:7<720::AID-JCC7>3.0.CO;2-X
30. I. Adamovic, M.A. Freitag and M.S. Gordon, *J. Chem. Phys.*, **2003**, 6725 (2015);
31. F. Furche and R. Ahlrichs, *J. Chem. Phys.*, **121**, 12772 (2004); https://doi.org/10.1063/1.1824903
32. H. Li, C.S. Pomelli and J.H. Jensen, *Theor. Chem. Acc.*, **109**, 71 (2003); https://doi.org/10.1007/s00214-002-0427-x
33. J. Perdew, M. Ernzerhof and K. Burke, *J. Chem. Phys.*, **105**, 9982 (1996); https://doi.org/10.1063/1.472933
34. V.F. Traven, L.I. Vorobjeva, T.A. Chibisova, E.A. Carberry and N.J. Beyer, *Can. J. Chem.*, **75**, 365 (1997); https://doi.org/10.1139/v97-042